

# Magneto-induced microstructure characterization of magnetorheological plastomers using impedance spectroscopy

Cite this: *Soft Matter*, 2013, 9, 7701

Yangguang Xu, Xinglong Gong,\* Taixiang Liu and Shouhu Xuan\*

An impedance spectroscopy (IS) method is employed to investigate the magneto-induced microstructure mechanism of magnetorheological plastomers (MRP). The IS of MRP with two typical particle distributions (isotropic and anisotropic) are compared and an equivalent circuit model is proposed to analyze the different impedance responses. It is found that the IS of anisotropic MRP is quite sensitive to the magnetic field and the electron diffusion effect will be restricted in the presence of a magnetic field. Furthermore, the conduction behavior of MRP in the presence of a magnetic field reveals the existence of elasticity in the polymer matrix. The influence of particle chain direction on the conductivity of anisotropic MRP with different particle contents is also investigated. Based on the experimental results, an equivalent method is developed to quantitatively characterize the anisotropy of MRP. With this method, the microstructure-dependent conduction mechanism of MRP can be presented more clearly.

Received 19th April 2013

Accepted 23rd May 2013

DOI: 10.1039/c3sm51072g

[www.rsc.org/softmatter](http://www.rsc.org/softmatter)

## 1 Introduction

Conductive polymer composites (CPC) are a kind of materials made by dispersing conductive fillers into an insulating polymer matrix, whose electrical conductivity has attracted great attention. A variety of conductive fillers such as graphene,<sup>1</sup> carbon nanotube,<sup>2</sup> graphite particles,<sup>3,4</sup> Ni particles,<sup>5,6</sup> and carbonyl iron particles,<sup>7–9</sup> have been chosen to investigate the electrical properties of CPC. Among them, Ni and carbonyl iron are typically soft magnetic particles, whose distribution in the polymer matrix can be changed by an external magnetic field (this kind of magneto-sensitive CPC is also denoted as magnetorheological elastomer, MRE). Both theoretical and experimental results demonstrate that the electrical properties of CPC are very sensitive to their microstructure (mainly referring to the conductive filler content and their distribution in the polymer matrix).<sup>10–12</sup> Therefore, a magnetic field becomes a direct controlling factor of electrical properties for the magneto-sensitive CPC by changing the distribution of conductive fillers. Due to the non-contacting nature of magnetic field control, the magneto-sensitive CPC shows fascinating application potential and the magneto-induced microstructure mechanism has been extensively investigated.<sup>10,12–15</sup>

However, the soft magnetic particles are fixed in the elastic polymer matrix after the composite is solidified. The microstructure of magneto-sensitive CPC (especially for the gaps between conductive particles) can hardly be changed by a

magnetic field, which restricts the magneto-controllability of electrical properties. To improve the electrical conductivity of MRE, an external loading was applied beforehand.<sup>3,9,16–18</sup> A consequent problem is that the geometry of the MRE sample will be significantly changed by the preloading. This geometry change, coupling with the magnetostriction effect, will complicate the investigation on the magneto-induced microstructure mechanism of magneto-sensitive CPC. The structured microstructure of a magnetorheological suspension (also denoted as a magnetorheological fluid, MRF) can be easily obtained by applying an external magnetic field,<sup>19,20</sup> but the structured microstructure will disappear immediately after the magnetic field is removed. While MRF is suitable for on–off control, continuous adjustable electrical properties is difficult to achieve. Recently, a new branch of magneto-sensitive CPC has been developed by dispersing soft magnetic conductive particles into a plastic polymer matrix, which was defined as magnetorheological plastomer (MRP).<sup>21</sup> The particles in MRP can rearrange some new microstructures driven by magnetic force. After the external magnetic field is removed, the particle distribution can still be kept in the plastic matrix. Moreover, because the loading cannot act on the plastic matrix, we can confine the MRP sample in an immovable space so that magnetic field becomes the only influencing factor of microstructure evolution without considering the geometry change induced by external loading and magnetostriction effect. The above characteristics make MRP an ideal candidate to investigate the magneto-induced microstructure mechanism of magneto-sensitive CPC. Making use of the electrical conductivity of filling particles, an impedance spectroscopy (IS) method can be chosen to characterize the magneto-induced microstructure evolution.

CAS Key Laboratory of Mechanical Behavior and Design of Materials, Department of Modern Mechanics, University of Science and Technology of China (USTC), Hefei, Anhui, China. E-mail: [gongxl@ustc.edu.cn](mailto:gongxl@ustc.edu.cn); Fax: +86 551 63600419; Tel: +86 551 63600419; [xuansh@ustc.edu.cn](mailto:xuansh@ustc.edu.cn); +86 551 63600419; +86 551 63606382

The IS technique is a powerful tool to characterize the electrical properties of materials and the interface behavior between electrode and electrolyte.<sup>22–25</sup> Normally, the IS experiment is implemented by applying an electrical perturbation (current or voltage) to the electrode–materials system and collecting the response signals. The most common and standard approach is to apply a single-frequency sinusoidal voltage to the electrode–materials system, then the IS can be defined as the frequency-dependent ratio of voltage to response current in the frequency domain by the use of Fourier transformation, which is actually the AC analog to resistance in DC.<sup>26</sup> Macdonald and Johnson believed that any intrinsic property that influences the conductivity of an electrode–materials system can be studied by IS.<sup>27a</sup> In addition, IS was classified as electrochemical IS (EIS) and everything else according to whether ionic conduction strongly predominates in materials. In particular, they pointed out that non-electrochemical IS measurement is still of great value in both basic and applied fields although EIS is the most rapidly growing branch of IS.<sup>28</sup>

In this study, we investigated the magneto-induced microstructure mechanism of MRP by an IS method. The IS of isotropic and anisotropic MRP in the absence of magnetic field were firstly compared and an equivalent circuit model was proposed to explain the structure-dependent impedance response. Then, the magneto-induced effect of MRP was studied and particularly the conductivities of MRP with different particle distributions under different magnetic fields were discussed. The influence of particle chain direction on the conductivity of MRP was finally considered. Based on the corresponding experimental results, an equivalent method was further developed to quantitatively characterize the anisotropy of MRP.

## 2 Experimental

### 2.1 Preparation of MRP

MRP samples were prepared by dispersing micrometer sized carbonyl iron particles (type CN, provided by BASF in Germany with an average radius of 6  $\mu\text{m}$ ) into a plastic polyurethane matrix. The synthetic process of polyurethane is from our previous work.<sup>21</sup> Five MRP samples with 40, 50, 60, 70 and 80 wt% fraction of iron particles, corresponding to 8.4, 12.1, 17, 24.2 and 35.4% in volume fraction, respectively, were prepared. These samples are denoted as MRP-40, MRP-50, MRP-60, MRP-70 and MRP-80, respectively, where the numbers after the names represent the weight fraction of iron particles in MRP.

### 2.2 Measurement system

As shown in Fig. 1, the IS measurement systems consist of four parts: magnetic field generator, electrode–material system (MRP sample and sample holder), Modulab® material test system (MTS, hardware), and data storage and analyzing system (software). A uniform and stable magnetic field can be obtained from the magnetic field generator by adjusting the current through the coil. 30 amperes of electricity will generate a 1000 mT magnetic field when the gap between two parallel

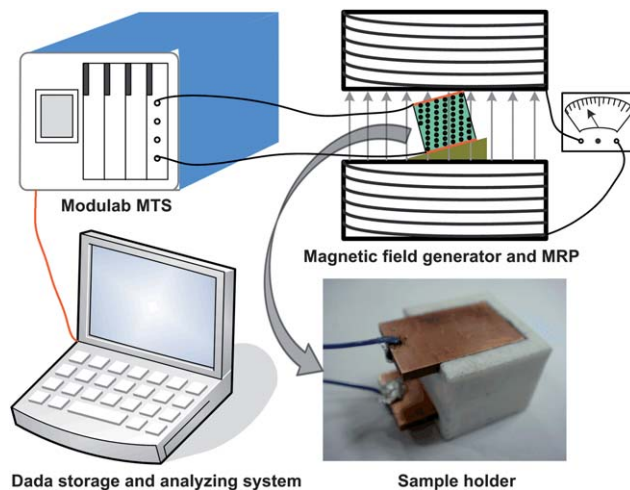


Fig. 1 Schematic of experimental setup for the IS measurements of MRP.

plates is 14 mm. It is worth noting that the magnetic field strength will decrease with decreasing of the gap between the parallel plates, so a tesla meter (type HT20, Shanghai Hengtong magnetic technology Co., Ltd, China) was used to measure the magnetic flux density with specific gap and current. The sample holder was placed on the surface of a wedge-shaped accessory with different angles of inclination. After a 1000 mT magnetic field was applied, MRP samples with a series of particle chain directions can be obtained. Due to the plastic property of MRP, as long as we design a 10 mm  $\times$  10 mm  $\times$  10 mm sample holder to load the MRP sample, the same geometry of MRP can be easily obtained (the reason for designing this special geometry will be discussed in Section 3.3). The framework of the sample holder is made by polytetrafluoroethylene for its good insulating property. Two identical copper sheets with smooth surface were chosen as electrodes connecting with the Modulab® MTS. The IS of MRP under various conditions were measured by the Modulab® MTS (Solartron analytical, AMETEK advanced measurement technology, Inc, United Kingdom), which is designed for testing the electrical properties of materials. In this study, only MAT (core module, 1 MHz) and FRA (Frequency Response Analyzer, 1 MHz) are used. The function of MAT is excitation voltage generation and response voltage/current measurement. The Modulab® MTS is controlled by the Modulab® software installed in PC. Various types of testing are available for Modulab® MTS. In addition, the Modulab® software can also store and analyze the experimental data.

### 2.3 Experimental condition

In this study, a continuous magnetic field ranging from 0 to 1000 mT was obtained by adjusting the coil current intensity of the magnetic field generator. The step type named “constant level” in the sub-item of “voltage controlled impedance” category was chosen. The type of AC stimulus applied to the sample is “frequency sweep” (the frequency sweep range was set from 0.1 Hz to 1 MHz) and no DC voltage was superimposed (*i.e.* 0 V was set in “DC level” option). All the measurements were implemented at room temperature.

Three preconditions (*i.e.* causality, linearity and stability) should be satisfied for a valid IS measurement. Because electronic conduction strongly predominates in MRP (no electrochemical process happens when testing), causality and stability are obviously satisfied for this pure physical impedance measurement. The impedance is supposed to be independent of the amplitude of the excitation signal if the response signal depends linearly on the perturbation. According to this principle, we designed a series of measurements to investigate the relationship between the amplitude of excitation voltage and the IS for MRP (Fig. 2). Good superposition for IS at the excitation voltages with different amplitudes were obtained (Fig. 2 shows the magnitude of IS), indicating the linear relationship between excitation signal and response signal can be satisfied when the amplitude of excitation voltage is smaller than 2 V. In addition, it is found that the data are unstable around the frequency of 50 Hz especially for the IS obtained at a smaller excitation voltage. This fluctuation phenomenon is induced by the resonance between the excitation voltage and the AC from the power source (the frequency of AC from the power source in China is 50 Hz). Higher excitation voltage can improve the stability of response signal. McKubre and Macdonald suggested that it is better to select the maximum value at which the response is independent of the amplitude of excitation signal.<sup>27b</sup> Therefore, 2 V was chosen as the amplitude of excitation voltage in this study.

### 3 Results and discussion

#### 3.1 Structure-dependent impedance of isotropic and anisotropic MRP

Mechanics method has been widely used to characterize the magneto-sensitive CPC with different particle distributions. The results demonstrated that particle distribution has significant influence on the mechanical properties.<sup>29–31</sup> However, the deformation induced by mechanics method will destroy the particle distribution. In other words, the particle distribution is

hard to be objectively reflected by the mechanical properties. When an electrical stimulus is applied to the sample, the response signal will be directly related to microstructure without destroying the particle distribution. Therefore, an electrical method is more suitable to investigate the structure-dependent mechanism than a mechanics method.

It is generally believed that there are two microstructure forms for MRE: isotropic and anisotropic. The magnetic particles disperse randomly in the isotropic MRE while a chain-like particle structure exists in the anisotropic one.<sup>32</sup> Similarly, the magnetic particles in MRP can also present random or structured distribution (here, we defined the anisotropic MRP as a sample exposed to a 1000 mT magnetic field for 20 min before measurement).<sup>33</sup> The frequency dependence of magnitude and phase angle of impedance are plotted in a Bode diagram, where the details of frequency response are displayed directly.<sup>28</sup> The Bode diagrams of MRP-80 with different particle distributions in the absence of a magnetic field are shown in Fig. 3. The magnitude of isotropic MRP is 2.058 times (average value in the whole frequency range) larger than that of anisotropic MRP in the whole frequency range, which indicates that the microstructure (*i.e.* the particle distribution) is a significant influencing factor on the electrical properties of MRP. For this reason, the impedance magnitude is a promising characterization parameter of the microstructure of MRP.

The same trends of magnitude and phase angle varying with frequency for isotropic and anisotropic MRP can also be found in Fig. 3, so the same model can be used to analyze their impedance responses. A Nyquist plot, plotting the real part and imaginary part of IS on the complex plane, is also widely used to investigate the interfacial properties and conduction mechanism of the electrode–materials system.<sup>22</sup> As Fig. 4 shows, both Nyquist plots of isotropic and anisotropic MRP present a straight line at low frequency followed by a semicircle at high frequency, but with different values.

An equivalent circuit was proposed to model the impedance responses of MRP in the absence of a magnetic field. As shown

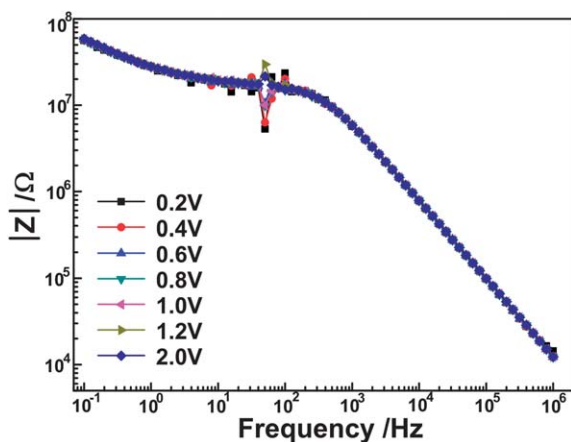


**Fig. 2** The magnitude of IS for MRP-80 at different amplitudes of excitation voltage. MRP-80 was subjected to a 1000 mT magnetic field for 20 min before measurement. The amplitude is actually the root mean square of the sinusoidal excitation voltage.

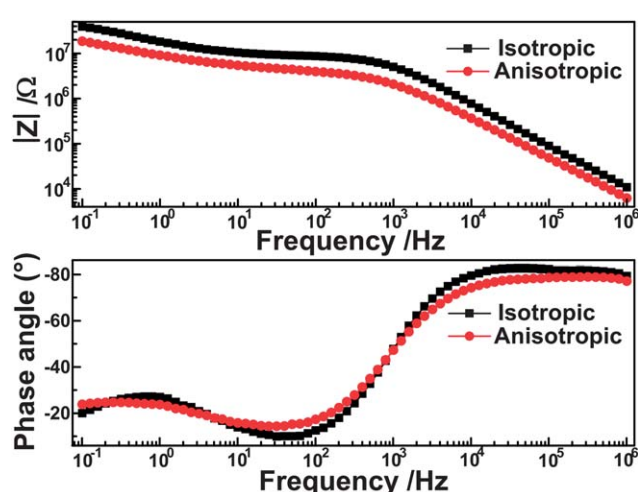


**Fig. 3** Bode diagrams of MRP-80 with different particle distributions (isotropic and anisotropic) in the absence of a magnetic field.

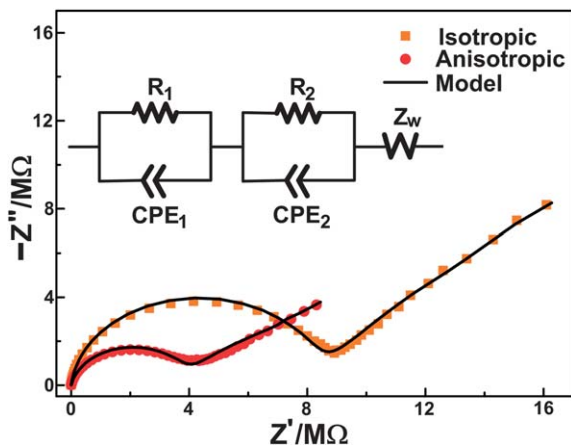


**Fig. 4** Nyquist plots of MRP-80 with different particle distributions (isotropic and anisotropic) in the absence of a magnetic field. The frequency range is  $1\text{--}10^6$  Hz. The inset is the equivalent circuit model used to fit the experimental results.

in the inset of Fig. 4, the equivalent circuit consists of a resistance ( $R_1$ ) in parallel with a constant phase element ( $Z_{\text{CPE}_1}$ ) and another resistance ( $R_2$ ) in parallel with CPE ( $Z_{\text{CPE}_2}$ ), along with a Warburg impedance ( $Z_{\text{W}}$ ). The impedance of CPE is defined as

$$Z_{\text{CPE}} = A^{-1}(j\omega)^{-P}, \quad (1)$$

where  $j = \sqrt{-1}$  and  $\omega$  represents the angular frequency.  $A$  and  $P$  are fitting parameters. CPE is usually used in place of a capacitor in an equivalent circuit where the experimental data cannot be well fitted by ideal circuit elements and is attributed to the presence of non-homogeneities in the electrode-materials system.<sup>23</sup> In fact, CPE can be interpreted as the general situations of ideal circuit elements: CPE is a resistance when  $P = 0$  while CPE becomes a capacitor when  $P = 1$ .<sup>25</sup> The Warburg impedance is the solution of the one-dimensional diffusion equation of a particle, which is mainly developed to model the charge diffusion phenomenon through a material in a finite-length region.<sup>28</sup> The expression of Warburg impedance is presented as

$$Z_{\text{W}} = \frac{R}{\sqrt{j\omega T}} \tanh \sqrt{j\omega T}. \quad (2)$$

The shape of impedance plots at low frequency is dominated by the two fitting parameters:  $R$  and  $T$ . The experimental data were transferred to Z-view software (Scribner Associates, Southern Pines, USA) and were analyzed by fitting to the equivalent circuit model as discussed above. The fitting results and related parameters are presented in Fig. 4 and Table 1, respectively.

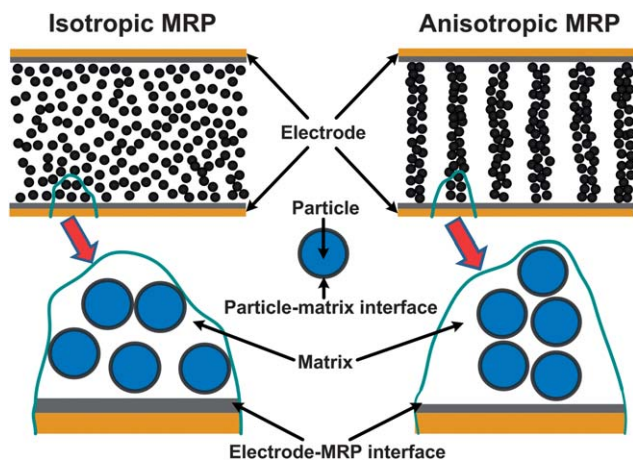
The equivalent circuit model fits well with experimental data (Fig. 4), indicating the proposed model is reasonable to analyze the microstructure-dependent impedance response of MRP. Therefore, the electrical elements in the proposed equivalent circuit model can be endowed with physical meanings related to the microstructure and interfaces of the electrode-MRP system. A schematic of MRP with different particle distributions and

corresponding interfaces are shown in Fig. 5. In the proposed model, we ignore the resistance of conductive particles and electrodes because they are much smaller than the resistances originating from the interface layers of electrode-MRP and particle-matrix. The interface layer of electrode-MRP can be regarded as a thin film consisting of a matrix and a few particles embedded in the consulting matrix. Obviously, the resistance of the electrode-MRP interface layer is smaller than the resistance originating from the matrix of MRP (the thickness of the MRP sample is larger than that of the interface layer of electrode-MRP). Therefore,  $R_1$  represents the electron transfer resistance coming from the interface layer of electrode-MRP while  $R_2$  represents the resistance of the matrix between adjacent particles in the direction of measurement. The surface asperities of electrode-MRP and particle-matrix interfaces are described by the CPEs in parallel with the corresponding resistance. In addition, The Warburg response should be attributed to the charge diffusion phenomenon through the whole electrode-MRP system (including the interfaces of electrode-MRP and particle-matrix).

After each electrical element in the equivalent circuit is defined, we can next analyze the structure-dependent impedance mechanism of MRP. It can be found from Table 1 that both  $R_1$  and  $R_2$  of isotropic MRP are larger than  $R_1$  and  $R_2$  of anisotropic MRP, respectively. Kchit and Bossis believed that the interfacial resistance determines the conductivity of CPC and electron transfer through the interface depends strongly on the gaps between particles and the roughness of the particle surface.<sup>12</sup> The same type of particle is used in the isotropic MRP and anisotropic MRP, so the influence of roughness on the interfacial resistance can be ignored. Therefore, it can be concluded that the differences of fitting parameters for isotropic MRP and anisotropic MRP are obviously attributed to the different particle distributions. As illustrated in Fig. 5, the gaps between adjacent particles which will dominate the value of  $R_2$  in anisotropic MRP are smaller than those in isotropic MRP. This explains that the conductivity of the matrix between adjacent particles in anisotropic MRP is better than that in isotropic MRP. The difference between isotropic and anisotropic MRP on  $R_1$  demonstrates that the particle distribution will affect the thickness of the electrode-MRP interface layer. It is possible that the insulating matrix between particles and electrode will be excluded during the formation of particle chains under an external magnetic field. However, the gap between two electrodes is fixed, so the interface layer of electrode-MRP will become thinner by the action of magnetic force and the structured configuration will be retained after the magnetic field is removed. For this reason, it is not difficult to understand that the resistance of the interface layer between electrode and MRP for isotropic MRP is larger than that of anisotropic MRP. We also notice that  $R_1$  of isotropic MRP is 2.15 times larger than that of anisotropic MRP while  $R_2$  of isotropic MRP is 4.72 times larger than that of anisotropic MRP. So it can be concluded that the particle distribution has a greater influence on the gap resistance between the adjacent particles in comparison with the interfacial resistance between electrode and MRP. The model

**Table 1** Fitting parameters obtained from the experimental data shown in Fig. 4

	$R_1/\Omega$	$A(Z_{CPE_1})$	$P(Z_{CPE_1})$	$R_2/\Omega$	$A(Z_{CPE_2})$	$P(Z_{CPE_2})$	$R(Z_W)$	$T(Z_W)$
Isotropic	$8.21 \times 10^6$	$3.71 \times 10^{-10}$	0.9515	$2.42 \times 10^7$	$2.64 \times 10^{-8}$	0.6392	$5.04 \times 10^6$	0.6489
Anisotropic	$3.81 \times 10^6$	$1.51 \times 10^{-10}$	0.9041	$5.12 \times 10^6$	$3.61 \times 10^{-8}$	0.6683	$4.46 \times 10^6$	0.6459

**Fig. 5** Schematic of MRP with different particle distributions and corresponding interfaces.

can well match with the experimental data by introducing CPE in the equivalent circuit, confirming the existence of non-homogeneity on the interfaces of electrode-MRP and particle-matrix. The huge difference of fitting parameters between  $Z_{CPE_1}$  and  $Z_{CPE_2}$  indicates that the roughness of interface between electrode and MRP is greatly different with that of the interface between particles and matrix. In addition, the parameters of Warburg impedance show little difference between isotropic and anisotropic MRP, then it can be deduced that the electron diffusion from conductive component (electrode and iron particle) to insulating component (polymer matrix) are hardly affected by the microstructure configuration of MRP.

### 3.2 Magneto-induced effect on the IS of MRP

Magnetic field controllability is the most fascinating property for magneto-sensitive material. The influence of magnetic field on the electrical properties of MRE has received increasing attention in recent years.<sup>3,7,16,34,35</sup> However, most of the results demonstrated that the magneto-induced effect on the electrical properties would be observed under a specific preloading. In other words, the electrical response signals contain the microstructure information induced by magnetostriction effect and external loading, which makes the investigation on magneto-induced microstructure mechanism of magneto-sensitive CPC more difficult. The magneto-induced microstructure can be decoupled from the deformation induced by preloading in MRP. Therefore, we can concentrate on the magneto-induced effect on the electrical properties when MRP is employed as the studied object.

The magneto-induced effect of anisotropic MRP-80 under different magnetic fields can be clearly observed from Fig. 6. The frequency-dependent magnitude decreases with increasing magnetic field when the frequency is lower than  $10^4$  Hz and the differences become less significant as the frequency increases. Interestingly, the difference of phase angle under different magnetic fields is obvious at high frequency ( $>10^3$  Hz) and all of the phase angles will tend to the same value as the frequency decreases. This frequency-dependent impedance response is quite different with the situation in the absence of magnetic field, indicating a different mechanism may be developed to explain the impedance response of MRP in the presence of a magnetic field.

The magneto-induced effect of anisotropic MRP-80 under the different magnetic fields can be more clearly presented by the Nyquist plots (as shown in Fig. 7). In comparison with Fig. 4, it is found that the most remarkable feature is that the straight line at low frequency disappears when MRP is exposed to a magnetic field. It is speculated that the Warburg response which manifests as a straight line at low frequency on Nyquist plots is restricted by the applied magnetic field. As we have mentioned above, the Warburg impedance mainly describes the electron diffusion phenomenon through the interfacial layer. The existence of a magnetic field hinders the electron diffusion through the interfacial layer, so the Warburg response will not be observed from the Nyquist plots. To further understand the magneto-induced effect on the impedance response of the electrode-MRP system in the presence of a magnetic field, a modified equivalent circuit model was then developed. As shown in the inset of Fig. 7, the Warburg impedance is removed compared with the equivalent circuit proposed in Fig. 4.

The fitting results can also be found in Fig. 7 and the related parameters are listed in Table 2. Good agreement between experimental data and the model indicates that the modified model is appropriate to explain the impedance mechanism of MRP in the presence of a magnetic field. In the modified equivalent circuit model,  $R_1$  and  $R_2$  represent the interfacial resistance of electrode-MRP and the resistance of the matrix between adjacent particles, respectively, the same physical meanings as the resistances shown in Fig. 4. By comparing the parameters listed in Tables 1 and 2, it is found that the resistances of MRP in the absence of magnetic are much larger than the corresponding ones under a magnetic field. For example,  $R_1$  and  $R_2$  of anisotropic MRP in the absence of a magnetic field are 158.7 and 27.1 times larger than  $R_1$  and  $R_2$  of anisotropic MRP under a 1000 mT magnetic field, respectively. This result demonstrates that even if stable particle chains have formed under an external magnetic field before measurement, the gaps between adjacent particles and

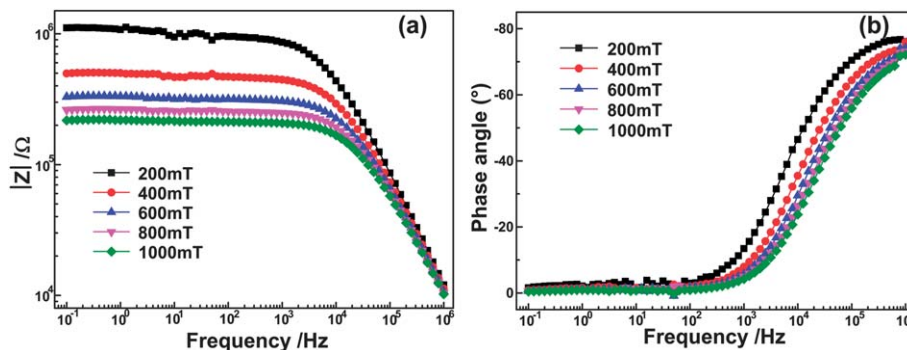


Fig. 6 Bode diagrams of anisotropic MRP-80 under different magnetic fields: frequency-dependent magnitude (a) and phase angle (b).

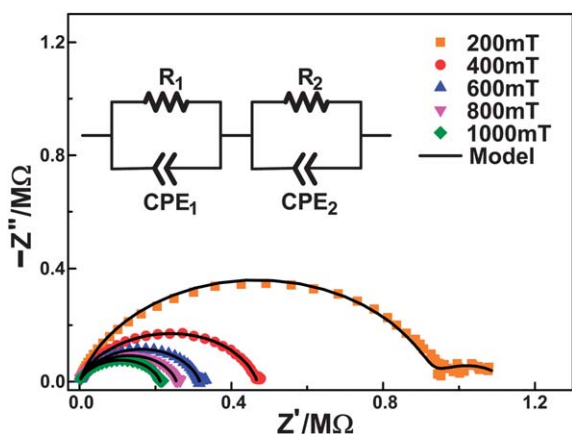


Fig. 7 Nyquist plots of anisotropic MRP-80 under different magnetic fields. The frequency range is 1–10<sup>6</sup> Hz. The inset is the equivalent circuit model used to fit experimental results.

the thickness of the interfacial layer between the electrode and MRP will decrease when the magnetic field is applied again. The magnetic interaction will reduce the gaps between adjacent particles and the thickness of interfacial layer between the electrode and MRP. Elastic deformation between adjacent particles will be generated because the MRP is confined in a fixed space. After the external magnetic field is removed, the elastic deformation of the matrix induced by magnetic interaction between adjacent particles will recover. The gaps between adjacent particles and the thickness of interfacial layer between the electrode and MRP increase accordingly. Therefore, the magneto-induced microstructure evolution of anisotropic MRP manifests that while MRP is not a complete plastic material, elasticity still exists in the polymer matrix.

These variations can be sensitively detected by impedance signals. Therefore, the differences of fitting parameters for anisotropic MRP actually reflect the variation in microstructure.

The resistances in the modified equivalent circuit model are sensitive to the gaps between adjacent particles and the thickness of interfacial layer between the electrode and MRP. It is found that  $R_1$  and  $R_2$  decrease with the increase of magnetic field strength, which demonstrates that the gaps between adjacent particles and the thickness of the interfacial layer between the electrode and MRP can be controlled by the magnetic field. In addition, it is worth mentioning that there is an obvious small semicircle (not a straight line) followed by a large semicircle in Fig. 7 for the MRP under a 200 mT magnetic field, which cannot be observed from the MRP under the other magnetic fields. This small semicircle is relevant with the interface layer between the electrode and MRP because the values of electrical elements which characterize the interfacial behaviors of MRP under 200 mT magnetic field ( $R_1$  and  $CPE_1$ ) are quite different from the others.

Bode diagram and Nyquist plot are different plotting approaches for the same IS. The relationship of the two approaches can be expressed by the following mathematical formula

$$Z(\omega) = |Z(\omega)|e^{j\theta(\omega)} = Z'(\omega) + jZ''(\omega), \quad (3)$$

where  $Z'$  describes the resistive behavior and  $Z''$  presents the capacitance component. Especially at low frequency, it is believed that the resistive response dominates in the whole IS. Here, the resistive components ( $Z'$ ) of IS at 0.1 Hz for MRP with different particle distributions under different magnetic fields are compared. As shown in Fig. 8, the conductivity of MRP with different preprocessing methods is significantly influenced by a magnetic field.

Table 2 Fitting parameters obtained from the experimental data shown in Fig. 7

Magnetic field/mT	$R_1/\Omega$	$A(Z_{CPE_1})$	$P(Z_{CPE_1})$	$R_2/\Omega$	$A(Z_{CPE_2})$	$P(Z_{CPE_2})$
200	19 8030	$5.50 \times 10^{-7}$	0.6343	92 8870	$1.66 \times 10^{-10}$	0.8357
400	43 648	$2.93 \times 10^{-10}$	0.8967	425 010	$2.76 \times 10^{-10}$	0.8270
600	27 216	$3.65 \times 10^{-10}$	0.8842	289 650	$3.06 \times 10^{-10}$	0.8237
800	26 456	$4.50 \times 10^{-10}$	0.8618	229 110	$3.27 \times 10^{-10}$	0.8229
1000	23 984	$5.15 \times 10^{-10}$	0.8506	188 920	$3.55 \times 10^{-10}$	0.8227

For the isotropic MRP,  $Z'$  will decrease sharply if it is pretreated by an external magnetic field before measurement (black data in Fig. 8). The larger the applied magnetic field, the smaller  $Z'$  is. This result is ascribed to the orientation arrangement of particles under an external magnetic field. The particle aggregation induced by the magnetic interactions of iron particles will decrease the gap between adjacent particles and the thickness of interfacial layer, so electrons will transfer through the electrode-MRP system more easily. The magnetic interactions are mainly decided by the magnetic field strength. That is to say, the magnetic field is an important influencing factor of the conductivity by controlling the particle distribution in MRP. With the increasing of magnetic field, the particle will gradually rearrange to form stable chain-like structures, which can be reflected from the variation of  $Z'$  under different pretreating magnetic fields. The isotropic MRP pretreated by a 1000 mT magnetic field is actually the anisotropic MRP which we have defined in Section 3.1. It is believed that stable chain-like structures are formed in anisotropic MRP. As for the other MRP which are pretreated by a magnetic field between 0 mT and 1000 mT, we defined them as low anisotropic MRP.<sup>21</sup> In low anisotropic MRP, the particles aggregate to form cluster structures along the magnetic field direction and are insulated by the polymer matrix from each other. Electrons move more easily in these MRP with cluster-like particle distribution than one with random particle distribution. Therefore, the conductivity of low anisotropic MRP is in between isotropic MRP and anisotropic MRP. The particles in MRE are fixed in the elastic matrix and are not easily moved by an external magnetic field. In comparison with MRE, the particle distribution in MRP can be easily adjusted by a magnetic field. The magneto-induced microstructure evolution has a great influence on the electrical properties of MRP, which make MRP possess more flexible magneto-

controllable properties. If the pretreated magnetic field is still kept when the measurement is carried out,  $Z'$  of isotropic MRP (red data in Fig. 8) will be smaller than that of MRP with the same pretreatment process in the absence of a magnetic field (black data in Fig. 8), this is another direct evidence which proves the existence of elasticity in the polymer matrix.

In the presence of a magnetic field,  $Z'$  of anisotropic MRP (blue data in Fig. 8) is smaller than that of isotropic MRP (red data in Fig. 8), but the difference in value trends to disappear with the increasing of magnetic field. Obviously, the particle distribution is the decisive factor for the difference in conductivity. Smaller  $Z'$  will be obtained in the MRP with higher anisotropic degree. If we observe the  $Z'$  of anisotropic MRP separately (the inset of Fig. 8), it is found that the conductivity of anisotropic MRP significantly decreases with the increasing of magnetic field, just like the magneto-induced effect on the conductivity of isotropic MRP. This magneto-induced effect on the conductivity was also found in MRE,<sup>36–38</sup> which is promising in terms of development of a magneto-sensitive sensor. However, it is worth noting that the mechanisms of magneto-induced conductivity for isotropic and anisotropic MRP are different. For anisotropic MRP, the variation of conductivity under different magnetic fields is attributed to the magnetostriction effect and the elasticity of the polymer matrix. In isotropic MRP, the rearrangement of iron particles induced by a magnetic field should also be considered when analyzing the magneto-induced effect on the conductivity.

### 3.3 The characterization on the anisotropy of MRP

The mechanical and electrical properties of anisotropic MRE will vary with the intersection angle between the measurement direction and the direction of particle chains (*i.e.* the direction of applied magnetic field before solidification).<sup>18,39,40</sup> Because the particle chains are fixed in the elastic matrix of MRE, different MRE samples with different particle chain directions should be prepared for the investigation on the relationship between particle chain direction and macroscopic properties. The microstructures of anisotropic magneto-sensitive CPC have been widely observed.<sup>33,41,42</sup> However, as far as we know, there is no effective method to quantitatively characterize the anisotropy of magneto-sensitive CPC by experimentation. Varga *et al.* measured the compressive moduli of MRE parallel and perpendicular to the direction of particle chains, respectively.<sup>39</sup> The magnetoresistances of MRE parallel and perpendicular to the direction of particle chains were compared by Mietta *et al.*<sup>18</sup> However, the results with the two methods are obtained under preloading, which cannot accurately reflect the microstructure information of MRE without deformation. The second problem as we have mentioned above is the comparison between two different samples will reduce the reliability of experimental results. As Fig. 9a shows, the ideal approach is comparing some physical quantity which contains the microstructure information in parallel and perpendicular to the direction of particle chains for the same sample. The ratio of this physical quantity obtained in different directions can be used to define the anisotropy of structured CPC. MRP is a more ideal candidate to substitute for

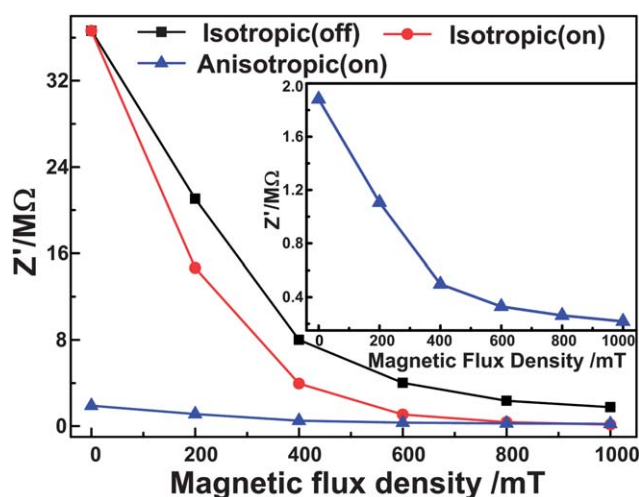


**Fig. 8** The resistive component of IS at 0.1 Hz for MRP-80 with different pre-processing methods under different magnetic fields. "Off" after the legend represents the measurement was carried out without a magnetic field while "on" after the legend represents the measurement was carried out under the present magnetic field (*i.e.* the corresponding magnetic field under the data point). Before measurement, the isotropic MRP was exposed to the present magnetic field for 20 min.

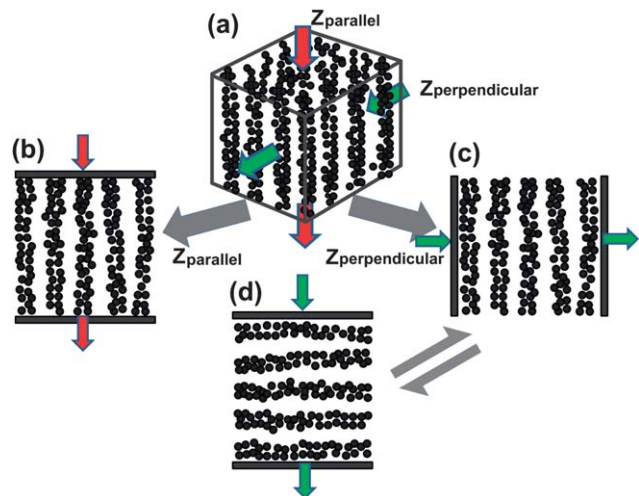


**Fig. 9** Schematic diagram of the characterization on the anisotropy of MRP. (a) The ideal measurement approach to determine the anisotropy of MRP; (b) IS measurement parallel with the particle chains; (c) IS measurement perpendicular with the particle chains; and (d) equivalent IS measurement perpendicular with the particle chains.

MRE to complete this research issue. Only one MRP sample is needed because the particle chain direction can be easily adjusted by applying an external magnetic field in different directions. What is more, the investigation on the influence of particle chain direction may provide us an effective method to quantitatively characterize the anisotropy of structured CPC.

The microstructure information of MRP without being destroyed can be sensitively detected by the IS method. The IS parallel with the particle chains can be easily obtained (Fig. 9b). Nevertheless, it is difficult to measure the IS perpendicular to the particle chain direction (Fig. 9c) because no electrode is designed on the side of MRP sample (the conductive electrode on the side of sample will affect the experimental result which is obtained parallel to the particle chain direction). Fortunately, an equivalent method can be developed to obtain the IS data of MRP perpendicular to the particle chain direction by making use of the moveable property of particles in MRP. As shown in Fig. 9d, the particles will rearrange to form a chain-like structure perpendicular to the measurement direction when applying the magnetic field in the corresponding direction. If the geometry of MRP sample is designed as a cube (in this study, the geometry of MRP sample is 10 mm × 10 mm × 10 mm), the IS in perpendicular to the particle chain direction (Fig. 9c) can be substituted by the IS obtained from Fig. 9d.

The measurement direction is regarded as the reference direction, the direction of particle chains can be then described by the intersection angle ( $\theta$ ) between the direction of particle chains and the measurement direction (as shown in the inset of Fig. 10). The IS of MRP with different particle chain directions in the absence of a magnetic field were measured.  $Z'$ , the resistive component of IS which reflects the conductivity of electrode-materials system, is employed as the characterization parameter. Further, the  $Z'$  ratio ( $R_\theta$ ) of anisotropic MRP with different particle chain directions is defined as

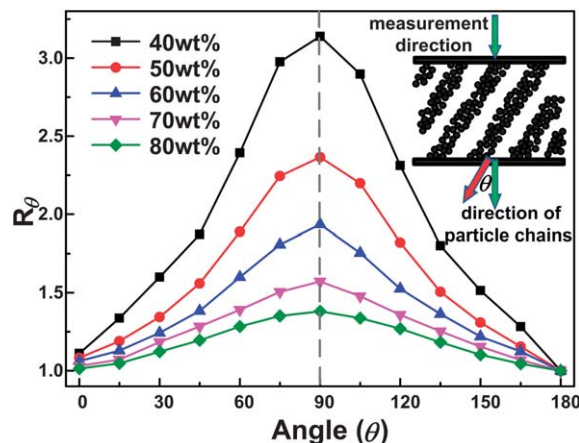


**Fig. 10**  $Z'$  ratio of anisotropic MRP with different particle contents in different particle chain directions. The meaning of the angle of horizontal axis represents the intersection angle between the direction of particle chains (*i.e.* magnetic field direction) and the measurement direction, as illustrated in the inset. A 1000 mT magnetic field was applied in the corresponding direction for 20 min before measurement and all of the measurements were carried out in the absence of a magnetic field.  $Z'$  presents the real part of impedance at 0.1 Hz.

$$R_\theta = \frac{Z'_\theta}{Z'_{\theta=180^\circ}}, \quad (4)$$

where  $Z'$  of anisotropic MRP when  $\theta = 180^\circ$  is the comparison object. In this way, the conductivity of MRP with different particle chain directions in comparison with that whose particle chain direction is in parallel with the measurement direction can be reflected from  $R_\theta$ . Fig. 10 shows that  $R_\theta$  reaches a maximum when the particle chain direction is perpendicular to the measurement direction (*i.e.*  $\theta = 90^\circ$ ). The further away from  $90^\circ$ , the smaller  $R_\theta$  becomes. In other words, the conductivity of MRP is highly dependent on the particle chain direction. The MRP shown in Fig. 9b ( $\theta = 0^\circ, 180^\circ$ ) shows better conductivity than the MRP shown in Fig. 9d ( $\theta = 90^\circ$ ), the conductivities of MRP with other particle distributions are in between them. As we have mentioned above, the conductivity of MRP depends on the interfacial layer of electrode-MRP and the gaps between particles in the direction of electron transfer. Obviously, the thickness of interfacial layer and the gaps between particles for MRP shown in Fig. 9d are larger than those of MRP shown in Fig. 9b, respectively. It is also found in Fig. 10 that  $R_\theta$  is relevant with particle content.  $R_\theta$  will increase with the decreasing of particle content for the same particle distribution. The  $R_\theta$  at  $90^\circ$  is the electrical parameter which can be used to quantitatively characterize the anisotropy of MRP. The approximate symmetrical distribution of  $R_\theta$  varying with  $\theta$  ( $90^\circ$  is the symmetrical axis) confirms that the definition of anisotropy by  $R_\theta$  is reasonable. Therefore, it is concluded that the anisotropy of MRP ( $R_\theta$  at  $90^\circ$ ) will decrease from 3.14 for MRP-40 to 1.38 for MRP-80. This result demonstrates that the higher the particle content, the smaller the differences on conductivity between parallel and perpendicular to the particle chain direction of MRP will become. That is to say, the particle distribution of MRP will trend to isotropic with increase of particle content under an external magnetic field.

## 4 Conclusions

The impedance responses of MRP with different particle distributions were systematically investigated. In the absence of a magnetic field, the particle distribution has a great influence on the IS of MRP. A proposed equivalent circuit model which agrees well with the experiment results revealed that the rearrangement of particles induced by a magnetic field will change the thickness of the interface layer of electrode-MRP and the gaps between adjacent particles along the direction of electron transfer, the conductivity of MRP will change accordingly. When an external magnetic field is applied, the electron diffusion effect will be restricted. A modified equivalent model without Warburg impedance can well describe the impedance behaviors of MRP under a magnetic field. Further analysis indicates that the magneto-induced effect originates from the elasticity existing in the polymer matrix. By comparing the conductivity of anisotropic MRP with different particle chain directions, an equivalent electrical method was developed to quantitatively characterize the anisotropy of MRP. With this method, it was found that for the MRP pretreated by an external magnetic field, the particle distribution will trend to isotropic with increasing of particle content.

## Acknowledgements

Financial support from the National Natural Science Foundation of China (Grant nos. 11125210, 11072234, 11102202) and the National Basic Research Program of China (973 Program, Grant no. 2012CB937500) are gratefully acknowledged.

## References

- 1 S. Stankovich, D. A. Dikin, G. H. B. Dommett, K. M. Kohlhaas, E. J. Zimney, E. A. Stach, R. D. Piner, S. T. Nguyen and R. S. Ruoff, *Nature*, 2006, **442**, 282.
- 2 T. Kimura, H. Ago, M. Tobita, S. Ohshima, M. Kyotani and M. Yumura, *Adv. Mater.*, 2002, **14**, 1380.
- 3 T. F. Tian, W. H. Li and Y. M. Deng, *Smart Mater. Struct.*, 2011, **20**, 025022.
- 4 I. Bica, *Mater. Sci. Eng., B*, 2010, **166**, 94.
- 5 J. S. Leng, X. Lan, Y. J. Liu, S. Y. Du, W. M. Huang, N. Liu, S. J. Phee and Q. Yuan, *Appl. Phys. Lett.*, 2008, **92**, 014104.
- 6 A. Kono, K. Shimizu, H. Nakano, Y. Goto, Y. Kobayashi, T. Ougizawa and H. Horibe, *Polymer*, 2012, **53**, 1760.
- 7 G. Bossis, C. Abbo, S. Cutillas, S. Lacis and C. Metayer, *Int. J. Mod. Phys. B*, 2001, **15**, 564.
- 8 I. Bica, *J. Ind. Eng. Chem.*, 2009, **15**, 233.
- 9 X. L. Zhu, Y. G. Meng and Y. Tian, *Smart Mater. Struct.*, 2010, **19**, 117001.
- 10 D. S. McLachlan, M. Blaszkiewicz and R. E. Newnham, *J. Am. Ceram. Soc.*, 1990, **73**, 2187.
- 11 J. S. Leng, W. M. Huang, X. Lan, Y. J. Liu and S. Y. Du, *Appl. Phys. Lett.*, 2008, **92**, 204101.
- 12 N. Kchit and G. Bossis, *J. Phys. D: Appl. Phys.*, 2009, **42**, 105505.
- 13 L. Y. Woo, S. Wansom, A. D. Hixson, M. A. Campo and T. O. Mason, *J. Mater. Sci.*, 2003, **38**, 2265.
- 14 W. Zhang, A. A. Dehghani-Sanij and R. S. Blackburn, *J. Mater. Sci.*, 2007, **42**, 3408.
- 15 D. S. McLachlan, *J. Electroceram.*, 2000, **5**, 93.
- 16 N. Kchit, P. Lancon and G. Bossis, *J. Phys. D: Appl. Phys.*, 2009, **42**, 105506.
- 17 N. Kchit and G. Bossis, *J. Phys.: Condens. Matter*, 2008, **20**, 204136.
- 18 J. L. Mietta, M. M. Ruiz, P. S. Antonel, O. E. Perez, A. Butera, G. Jorge and R. M. Negri, *Langmuir*, 2012, **28**, 6985.
- 19 M. Sedlacik, V. Pavlinek, M. Lehocky, A. Mracek, O. Grulich, P. Svracinova, P. Filip and A. Vesel, *Colloids Surf., A*, 2011, **387**, 99.
- 20 M. Sedlacik, R. Moucka, Z. Kozakova, N. E. Kazantseva, V. Pavlinek, I. Kuritka, O. Kaman and P. Peer, *J. Magn. Magn. Mater.*, 2013, **326**, 7.
- 21 Y. G. Xu, X. L. Gong, S. H. Xuan, W. Zhang and Y. C. Fan, *Soft Matter*, 2011, **7**, 5246.
- 22 J. T. S. Irvine, D. C. Sinclair and A. R. West, *Adv. Mater.*, 1990, **2**, 132.
- 23 E. Katz and I. Willner, *Electroanalysis*, 2003, **15**, 913.
- 24 R. Amin, C. T. Lin, J. B. Peng, K. Weichert, T. Acarturk, U. Starke and J. Maier, *Adv. Funct. Mater.*, 2009, **19**, 1697.
- 25 A. Munar, A. Sandstrom, S. Tang and L. Edman, *Adv. Funct. Mater.*, 2012, **22**, 1511.
- 26 D. C. Sinclair, *Bol. Soc. Esp. Ceram. Vidrio*, 1995, **34**, 55.
- 27 (a) J. R. Macdonald and W. B. Johnson, in *Impedance Spectroscopy Theory, Experiment, and Applications*, ed. E. Barsoukov and J. R. Macdonald, John Wiley & Sons, New Jersey, 2nd edn, 2005, Ch. 1; (b) M. C. H. McKubre and D. D. Macdonald, in *Impedance Spectroscopy Theory, Experiment, and Applications*, ed. E. Barsoukov and J. R. Macdonald, John Wiley & Sons, New Jersey, 2nd edn, 2005, Ch. 3.
- 28 J. R. Macdonald, *Ann. Biomed. Eng.*, 1992, **20**, 289.
- 29 T. Mitsumata and S. Ohori, *Polym. Chem.*, 2011, **2**, 1063.
- 30 G. J. Liao, X. L. Gong, S. H. Xuan, C. Y. Guo and L. H. Zong, *Ind. Eng. Chem. Res.*, 2012, **51**, 3322.
- 31 Y. G. Xu, X. L. Gong, S. H. Xuan, X. F. Li, L. J. Qin and W. Q. Jiang, *Soft Matter*, 2012, **8**, 8483.
- 32 L. Chen, X. L. Gong and W. H. Li, *Smart Mater. Struct.*, 2007, **16**, 2645.
- 33 X. L. Gong, Y. G. Xu, S. H. Xuan, C. Y. Guo, L. H. Zong and W. Q. Jiang, *J. Rheol.*, 2012, **56**, 1375.
- 34 I. Bica, *J. Ind. Eng. Chem.*, 2010, **16**, 359.
- 35 C. H. Wan, X. Z. Zhang, X. L. Gao, J. M. Wang and X. Y. Tan, *Nature*, 2011, **477**, 304.
- 36 Z. H. Guo, S. Park, H. T. Hahn, S. Y. Wei, M. Moldovan, A. B. Karki and D. P. Young, *Appl. Phys. Lett.*, 2007, **90**, 053111.
- 37 X. J. Wang, F. Gordaninejad, M. Calgar, Y. M. Liu, J. Sutrisno and A. Fuchs, *J. Mech. Des.*, 2009, **131**, 091004.
- 38 I. Bica, *J. Ind. Eng. Chem.*, 2012, **18**, 483.
- 39 Z. Varga, G. Filipcsei and M. Zrinyi, *Polymer*, 2006, **47**, 227.
- 40 A. Boczkowska, S. F. Awietjan, S. Pietrzko and K. J. Kurzydowski, *Composites, Part B*, 2012, **43**, 636.
- 41 W. H. Li, Y. Zhou and T. F. Tian, *Rheol. Acta*, 2010, **49**, 733.
- 42 J. K. Wu, X. L. Gong, Y. C. Fan and H. S. Xia, *Soft Matter*, 2011, **7**, 6205.